TheATLAS

Detecting and Discriminating Small Arms Fire Using Neural Networks: Tools to Mitigate Urban Gun Violence

Simeon Symeonidis*[1] *and Alan Barhorst*[2]*, [1] *Trackingpoint, 17431 Bristow Dr., Galveston, TX 77552, Email: symeonidis@ymail.com;* [2] *Texas Tech University, Mechanical Engineering, Lubbock TX, 79409, Email: alan.barhorst@ttu.edu*

doi: 10.22545/2014/00058

This paper outlines a two-layer neural network used to declare small arms fire based upon a temporal, electro-magnetic signature. The neural network discriminates targets from noise and common clutter sources, such as sun glints. This neural network is compared against a baseline algorithm derived from traditional detection and discrimination processing. A simulation is performed to evaluate the performance of each approach, and the simulation results are captured via a Receiver Operator Curve. This algorithm, in conjuction with a high-rate infrared sensor, would provide law-enforcement a tool for mitigating urban violence.

Keywords*:* law-enforcement, small arms fire indication systems, temporal processing, neural networks, infrared systems.

1 Introduction

The National Education Association Health Information Network states that, in the United States, over eighty people die from gun violence each day [1]. A partial technical solution to this problem would be to deploy a small arms fire indication system. Even though indication systems cannot prevent gun use, they can quickly locate a gunfire event, aiding law-enforcement in the apprehension of suspects. However, small arms gunfire is a difficult event to detect because of its limited signal, small duration, and small volume. There is also the additional challenge of competing common natural phenomena, such as sun glints (electro-optical systems) and thunder (acoustic systems) which can be misinterpreted as small arms fire. Although there exists small arms fire indication systems for military applications, creating a law enforcement system is technically more challenging, since these class of systems are detecting weapons with smaller signatures [2]. In military operations, larger assault rifles (e.g. AK-47 and M-16) are prevalent and pose the main threat, whereas in law enforcement applications, smaller handguns are a larger threat. Also, in the military, guns are often fired in semi-automatic or fully-automatic mode, but in law enforcement applications, an event with only one shot is the typical scenario. Multiple shots per small arms fire event increase the amount of signal and can provide an extended temporal signature for use in discrimination.

Notionally, there are two types of small arms indication systems. The first is a high-altitude

surveillance system that can identify and report weapons fire over a large field-of-regard (FOR). This information is crucial for removing repeat gun violence offenders from the streets [3]. One design challenge associated with this system is to identify high-bandwidth processing that can compliment the high-performance, large-FOV sensor. The processing needs to report information reliably, meaning that there is a high target probability of detection (PD) and a low false alarm rate (FAR). Due to the high processor data bandwidth needed to process information from high-resolution sensors (i.e. high angular resolution is needed to detect distant targets over and extended ground areas), these systems would also require algorithms that can efficiently use available processing resources, whether it be an Application Specific Integrated Circuits (ASIC), Field Programmable Gate Arrays (FPGA), or analog processing embedded within the detector Read Out Integrated Circuit (ROIC) [4].

The second type of small arms fire indication system would be used by teams that routinely engage in hostile conditions, e.g. Special Weapons and Tactics (SWAT) teams, to quickly determine if there is small arms fire and its source. This will provide the information needed to ensure the safety of the public and those who serve the public. It is even more important for these locally-deployed systems to have a high PD and a low FAR since inaccurate information can result in injuries and death. Although these systems do not require the same processing bandwidth as the wide-coverage surveillance systems, these systems often have stringent cost, size, weight, and power constraints, which limit the amount and type of processing that can be implemented. As a result, these systems also need to efficiently use processing resources [5].

In either case, the system needs algorithms that operate reliably while minimizing processing resources. Traditional algorithms for detection and discrimination exist, but the hypothesis is that neural networks can be used to improve overall system performance and increase processing efficiency [6 , 7]. This would enable systems that better address the needs of law enforcement. This paper is on the assessment of how neural networks can be used for law-enforcement small arms fire indication systems and how they compare to traditional algorithms. To limit the scope, the focus will be on how neural networks can improve probability of declaration (PD) and probability of a false alarm (PFAR). PFAR can be translated into FAR by multiplying it with the sensor bandwidth. Electro-optical systems will be assumed since they provide better line-of-sight information, they do not require an active transmitter, and can provide better overall performance [8]. To discriminate between targets and clutter, e.g. sun glints, spectral, temporal, or spatial signatures can be used. This paper will focus on temporal processing, since it does not require the use of spectral filters tuned to the target and can achieve large FOR given detector sizes available today [4].

2 Background

Figure 1 below provides an overview of small arms, their components, and their ammunition. The cartridge has a projectile, propellant, primer, which is enclosed in the case. First, the cartridge is loaded into the chamber. In the chamber, the cartridge will be struck by the firing pin, which in turn lights the primer. The primer will burn the propellant, which will create gases that expand fourteen thousand times its volume forcing the bullet down the barrel out the muzzle, and the hot cartridge case will be ejected out of the chamber [9].

Firearms are weapons that are based upon the principles of kinetics: they use force to propel projectiles toward targets. Higher speeds and larger projectile masses transmit more energy, allowing for greater damage, longer ranges, and better accuracy. To generate these forces, a propellant is ignited in the chamber, but due to various inefficiencies, only 30% of the propellants energy is transferred to the bullet; the rest is dissipated by other means. These inefficiencies allow for small arms fire detection systems, not based on detecting bullets, to operate. Generally, more propellant allows for greater force to be imparted to the projectile, which causes more damage, but also results in more energy dissipated to the environment and hence a stronger signature to be detected. A more detailed description can be found in the book by Klingenberg and Heimerl [10].

There are three major EM events associated with gunfire. The first, primary flash, consists of high-speed, high-energy propellant exiting the muzzle. Primary flash is an extremely brief event that is difficult to detect. The second, intermediate flash, occurs further outside the muzzle. Intermediate flash is a result of high pressure gases and propellant decel-

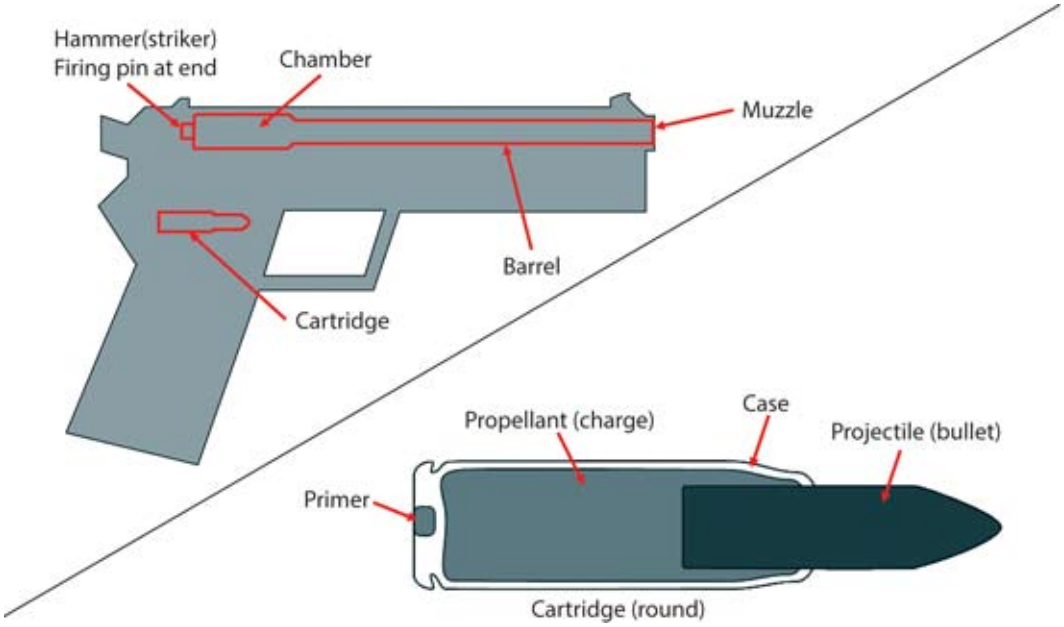

Figure 1: Firearm construction and terminology.

erating and decompressing as it leaves the gun. The last, secondary flash consists of the high-temperature exhaust gases and propellant mixing with the atmosphere and cooling down. Since this event has the longest duration, it is likely to be the easiest for sensors to detect. As a result, this study will attempt to model this specific phenomenon. The three EM events are captured in Figure 2 [10].

It is common in the IR modeling community to use Plank's Blackbody Law to model radiance, energy, per area, per time, per solid angle to determine signal intensity. Plank's Blackbody Law, which determines a perfect emitter, spectral radiance, $L_{bb\lambda}$, at temperature, T, and at wavelength, λ, is [11].

$$L_{bb\lambda}(T,\lambda) = \frac{2 \cdot h \cdot c^2}{\lambda^5} \cdot \frac{1}{e^{\frac{h \cdot c}{\lambda \cdot k \cdot T}} - 1} \left(\frac{\text{watt}}{\text{cm}^2 \cdot \text{sr} \cdot \mu\text{m}} \right) \tag{1}$$

Where k is the Boltzmann constant, h is the Plank constant, and c is the speed of light. To understand the energy radiated by a blackbody in a waveband bounded by the lower limit, λ_1, and the upper limit, λ_2, the spectral signature, provided by Plank's Law is integrated over the region of interest:

$$L_{bb}(T,\lambda_1,\lambda_2) = \int_{\lambda_1}^{\lambda_2} L_{bb}(T,\lambda) d\lambda \left(\frac{\text{watt}}{\text{cm}^2 \cdot \text{sr}} \right) \tag{2}$$

Planks Blackbody Law can be used to provide a first-order model of the spectral response and radiance of all the objects needed for this article: a small arms flash, background materials, and sun glints. The gases and particulates temperatures leaving a gun muzzle have been measured to be anywhere from 1000 to 1500 K. Grant and Hardy used a small emissivity of 0.05-0.1 to estimate the radiance of small arms flash [12], which is utilized herein. This emissivity, in combination with the 1000 K temperature, the lower-end exhaust temperature, was used to generate the small arm flash greybody curve presented in Figure 3. Notice that most of the flash energy is in the mid-wave infrared (IR), 3-5 μm, and short-wave IR, 1-3 μm, spectrum. A mid-wave IR (MWIR) system will be assumed for this work because it is consistent with military small arms fire indication system [2].

Next, the background objects can be modeled as blackbodies, i.e. emissivity of one, at ambient temperature, e.g. 300 K, plus or minus several degrees. This spectral response curve is also plotted in Figure 3. Notice that despite small arms flash limited emissivity, the small arms flash still has considerably more energy than background objects in the aforementioned spectra. This demonstrates that in the MWIR spectrum, small arms flash has more energy than background material. As a result, small arms flash will appear as a signal with a amplitude larger

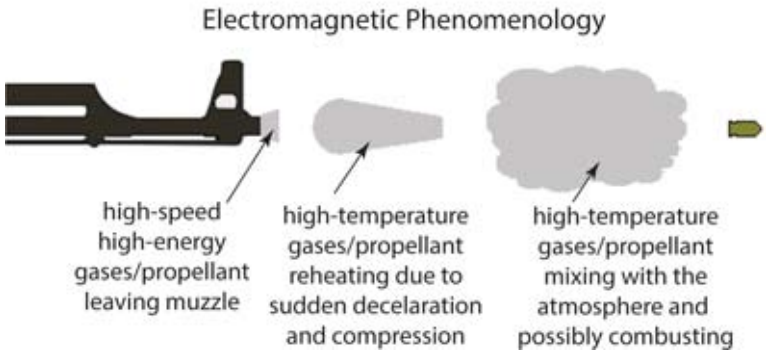

Figure 2: Phenomenology.

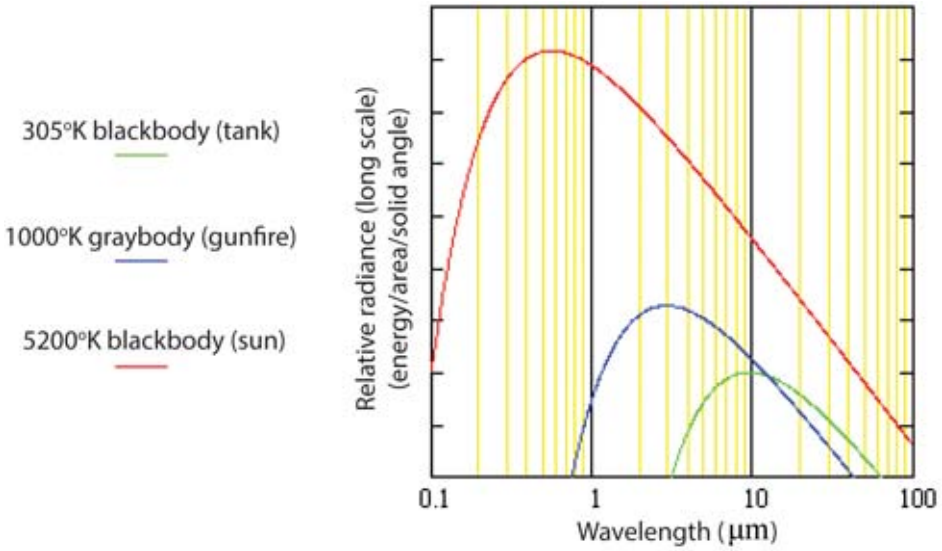

Figure 3: Blackbody spectral signatures.

than its surrounding background material. Lastly, the sun can be modeled via a 5200 K blackbody; if the object is reflective, the sun glint spectral energy response can also be approximated by a 5200 K blackbody, minus atmospheric effects. This is the third curve captured in Figure 3. Notice that sun glints have more energy than flash throughout the EM spectrum. This prohibits using energy levels exclusively for detection and discrimination. This point will be developed further below [12].

Spera and Figle provided a small arms MWIR radiant intensity measurement of 5 watts/sr to 100 watts/sr in their work on sniper detection systems using uncooled sensors [13]. It is not clear what value is correct for the radiant intensity in this application, but the assumption that law enforcement needs to detect smaller weapons such as handguns is made. This assumption places target intensities somewhere near the bottom of the spectrum, i.e. 10 watts/sr. Spera and Figle also provided a small arms flash size and duration, which can be used to derive total and average flash energy [13]. This information is summarized in Table 1.

Given the estimates provided by Spera and Figle, it can be inferred that small arms flash is an extremely intense event with a small spatial size and short time duration. Using common analogies, small arms flash is as intense as four, 100-watt incandescent light bulbs (calculation assumes 2.5% luminance efficacy, ratio of the power generated in the visible spectrum over the total power consumed), but fifteen times shorter than a single humming bird wing flap, and occupying the volume of a human toddler [14, 15]. This is consistent with the phenomenology that extremely hot emitted exhaust gases and unspent propellant remain close to the muzzle and do not

Table 1: Flash radiometric intensity.

flash duration = 1.5ms

flash size (centroid) = 0.732m x 0.305m x 0.305m

		Spatial Domain	
		Low Resolution	High Resolution
Temporal Domain	Low Resolution	15 mJ/sr	8.57-20.56 μJ/cm²sr
	High Resolution	10 watts/sr	5.72-13.71 mwatts/cm²sr

take much time to reach the temperature/pressure of the surrounding atmosphere.

To provide a comparison point, a target often modeled using infrared sensors is a tank. Using the assumptions stated in the infrared modeling tool user manual of the U.S. Army, NVTherm [16], in a 300 K background, at night, in Southwest Asia, a tank can be modeled as an 11.6 m^2 (125 ft^2), 305 K blackbody. Although the tank radiance in the MWIR spectrum is lower than a flash, i.e. $2.217x10^{-4}$ watt/cm^2/sr, the tank radiates the same amount of energy as a flash within 2.44 ms-171 ms. One way to view this is that although the instantaneous energy is large compared to other phenomenon, its relatively small size and short duration can make it a harder event to detect. It is this reason that to attain similar coverage, a small arms indication system requires higher performance sensors than systems designed to detect and discriminates targets that remain in the field of view for an extended period. Higher performance is often achieved through higher resolution detectors, and this increased sensor performance often translates to higher processing bandwidth; hence the larger emphasis on using processing resources efficiency compared to systems that detect and discriminate objects like vehicles, people, etc [16].

Plank's Blackbody Law only models radiance. The radiance can be integrated over the projected area to determine the radiant intensity. This can be used to determine the radiant intensity of a sun glint. This allows the direct comparison of intensities, imaged by an unresolved sensor, of flash and sun glint. To model radiant intensity, unresolved sensors will be assumed. The radiance of a 5200 K blackbody in the MWIR spectrum is 22.7 watt/cm^2/sr. The sun diameter is about $1.396x10^9$ m, and the distance is about $4.56x10^{10}$ m [17]. Using the small angle approximation, the apparent size of the sun from the earth is 0.923 cm. Assuming that the sun glint has the same intensity and apparent size this would translate to a radiant intensity of 18.802 watt/sr. This means that the instantaneous energy of a glint is close to two time that of a flash. This information will be used to generate temporal signature of flash and sun glints in this work [18].

This gunfire flash event is characterized by a rapid increase of exhaust volume leaving the muzzle, followed by a decrease in exhaust temperature, creating an IR temporal signature that resembles Figure 4. Intensities are depicted relative to noise levels and durations relative to frame rate. The curve in Figure 4 only provides an estimate, and the temporal profile was not validated by experiment. The absolute intensity and duration was omitted since doing so would require a priori knowledge of the performance, atmospheric transmission, etc, and is not needed for this processing architectures evaluation. What is important and is included in the figure is the flash intensities relative to sun glints [10]. From a modeling perspective, sun glint can be modeled as a "spotlight." If the platform is flying through that spotlight, the sensor will be collecting photons from materials reflecting solar energy; otherwise the sensor will not be receiving energy. This will create a signature that roughly resembles a square pulse (see Figure 4). The pulse duration will be a function of the platform altitude and velocity, but for this work, it will be assumed that the sun glint pulse duration will be the same as the flash duration. This is a realistic assumption for some applications and will provide a challenging stimulus for signal detection and discrimination [18].

The stimuli, which include all the aforementioned information, are captured in Figure 4 and will be used to evaluate neural networks for this application. To produce reliable small arms fire indications, the

processing would have to perform two functions: detect a signal and noise and to discriminate flash from temporal phenomenon, such as sun glints.

3 Approaches

Two different approaches will be evaluated in this paper: an algorithm based upon traditional digital signal processing techniques and a two-layer neural network.

3.1 Matched Filter Based Approach

The approach based on traditional processing consists of two parts: a filter that separates signal from noise and another filter that separates signal from clutter. Filtering signal from noise is insufficient, by itself, because clutter, such as sun glints, can have more energy, after filtering, than small arms flash. Filtering signal from clutter is not sufficient due the noise level, cause by variation in the background signal and random processes in the sensor, and the limited temporal samples per event. In these situations, noise can easily cause false alarms. The traditional approach uses a matched filter, an optimal filter for detecting a signal in noise, provided that the noise can be characterized using second-order statistics, to separate the signal from noise. The definition of a simplified matched filter is [19]:

$$O_{\mathrm{SN}} = \bar{S}^T M^{-1} \bar{Z} \tag{3}$$

Where s is the known signal vector, M is the noise covariance matrix, z is the input data vector, and $\mathrm{O_{SN}}$ is the output of the filter. Superscript T is used to denote a vector transpose operation and superscript -1 is used to indicate a matrix inversion. If the input data vector, z is weak or wide-sense stationary, meaning that the first and second order moments do not vary between elements, and each element is independent of each other, the noise covariance matrix becomes the identity matrix multiplied by a constant. This further simplifies the matched filter to the filter given by:

$$O_{\mathrm{SN}} = \bar{S}^T \bar{Z} \tag{4}$$

A threshold, $\mathrm{T_{SN}}$, can be applied to the filter output, $\mathrm{O_{SN}}$, to declare the existence of a signal. The set of all declared signals in noise is given by:

$$H_{\mathrm{SN}} = \{O_{\mathrm{SN}} : O_{\mathrm{SN}} > T_{\mathrm{SN}}\} \tag{5}$$

T_{SN} can be adjusted to trade $\mathrm{P_D}$ and $\mathrm{P_{FAR}}$.

To separate signal from clutter, the input data signal, z, vector can be normalized to create a signature that declares based upon the temporal profile of the signal. A matched filter can then be applied to the normalized signal to determine how close the temporal shape of the filter matches the known signal. This filter is given by:

$$O_{\mathrm{SC}} = \frac{\bar{S}^T \bar{Z}}{\sum \bar{Z}} \tag{6}$$

Where $\mathrm{O_{SC}}$ is the output of the filter optimized for signal to clutter. A different threshold, $\mathrm{T_{SC}}$, can be applied to the filter output, $\mathrm{O_{SC}}$, to declare the existence of a signal in clutter. $\mathrm{T_{SC}}$ will also impact $\mathrm{P_D}$ and $\mathrm{P_{FAR}}$. The set of all declared signals in clutter is given by:

$$H_{\mathrm{SC}} = \{O_{\mathrm{SC}} : O_{\mathrm{SC}} > T_{\mathrm{SC}}\} \tag{7}$$

The filters specified in Equations 3 and 5 can be combined to discriminate signal from both noise and clutter. This algorithm, which serves as the baseline in this work, is captured as:

$$H_{\mathrm{S}} = H_{\mathrm{SC}} \cup H_{\mathrm{SN}} \tag{8}$$

An illustration of the baseline algorithm using a high-rate, low-noise signal is presented in Figure 5. The input signal,z, consist of white Gaussian noise, a small arms flash signal (left) and a sun glint signal (right). Notice that the filter, optimized for detecting signal in noise, $\mathrm{H_{SN}}$, declares both the flash and glint and a filter optimized for detecting signal in clutter,$\mathrm{H_{SC}}$, declares signals consisting of only noise, independent of threshold values. However, combining these filters produces a robust algorithm that declares flash and not sun glint with high reliability as is shown below.

3.2 Neural Network Based Approach

The neural network approach that will be taken for small arms detection and discrimination is a two-layer neural network. The first layer will consists of two neurons, one that is matched to small arms flash, $\mathrm{O_{SN}}$ and the other matched to a sun glint, $\mathrm{O_{GLINT}}$. The equation for a matched filter, assuming weak or wide sense stationary and independent samples, is presented in Equation 2. These neurons will be connected to a third neuron, OS. In the second-layer neuron, the flash matched filter input will be

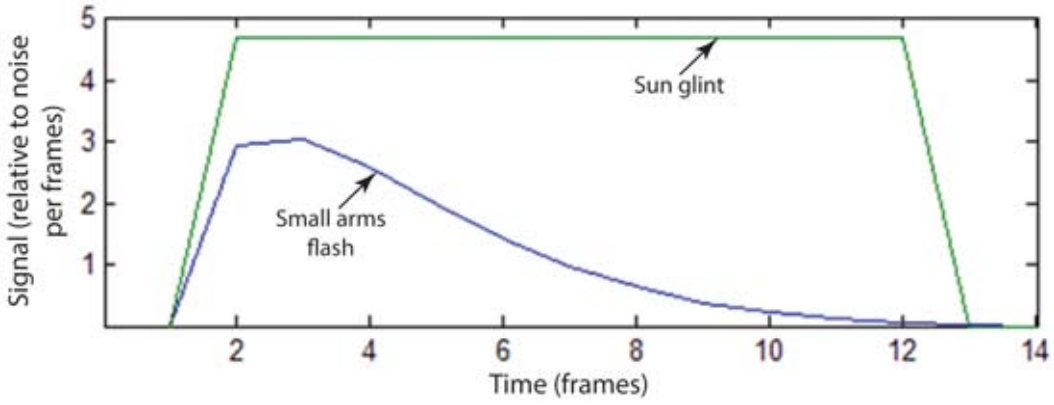

Figure 4: Small arms declaration neural network.

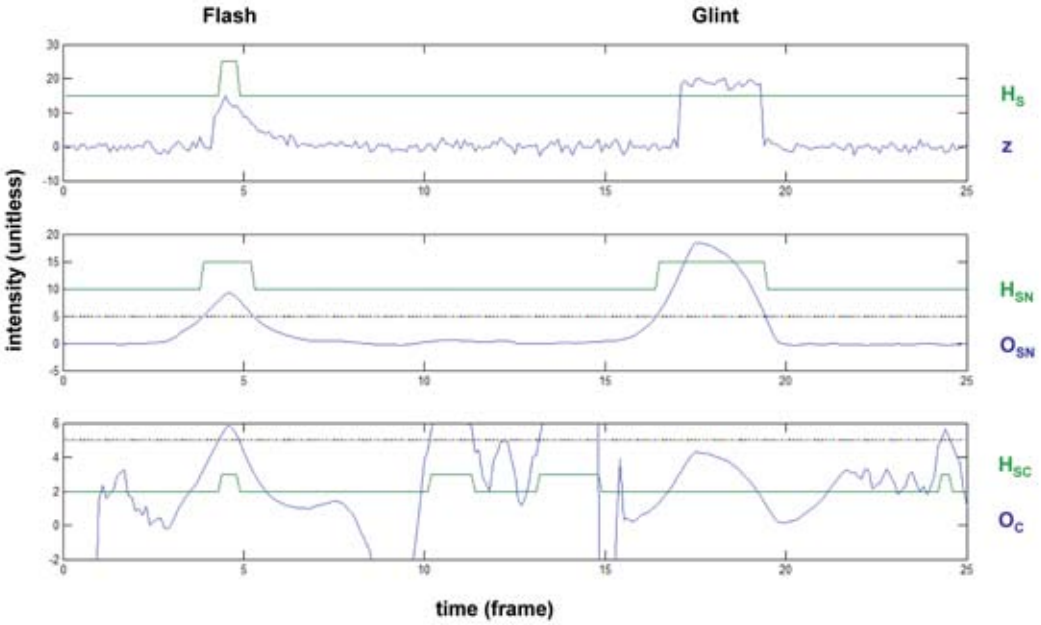

Figure 5: Baseline algorithm simulation.

excitatory, i.e. the weight, W_{SN}, will be positive, the glint matched filter input will be inhibitive, i.e. the weight, W_{GLINT}, will be negative, and the bias, B, can be either positive or negative. The weights and the bias for the third neuron can be adjusted to trade P_D and P_{FAR}. This neuron operation is captured in Equation 9.

$$O_s = W_{SN} \cdot O_{SN} - W_{GLINT} \cdot O_{GLINT} + B \quad (9)$$

The two-layer neural network is summarized in Figure 6. The boxes with z^{-1} represent unit delays needed to synchronize the temporal matched filters inputs. If the neuron output, O_S, is positive, a declaration will be made. One aspect that differentiates the neural network from the algorithm based on traditional signal processing is the inclusion of the clutter signal, which allows the algorithm to be tuned to eliminate specific phenomena. The hope is that this design feature can be used to improve performance. Another difference is the existence of only one threshold, compared to the two needed for the baseline. Having to pass two distinct criteria through an algorithm can make achieving a high target PD, i.e. greater than 95%, more difficult. Also, having only one threshold may simplify adjusting the algorithm parameters.

An illustration of the neural network, using a

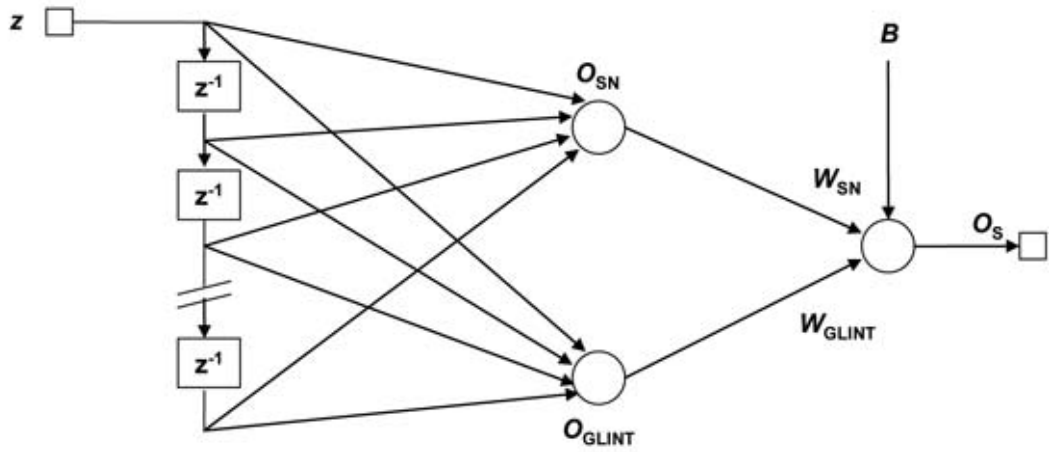

Figure 6: Small arms declaration neural network.

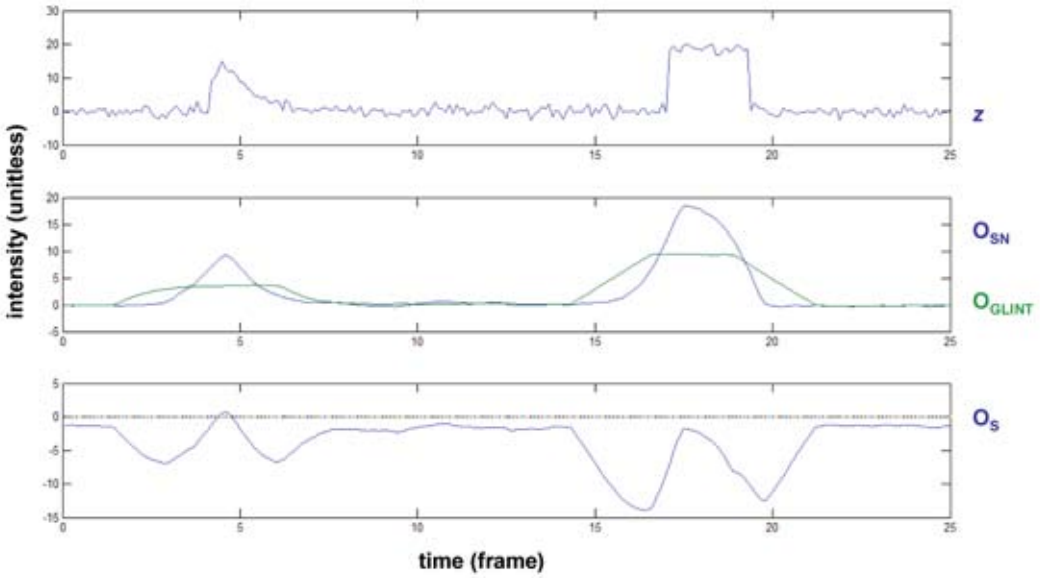

Figure 7: Neural network simulation.

high-rate, low-noise signal is presented in Figure 7. The input signal, z, is the same signal used to simulate the baseline algorithm. Notice that the glint matched filter, O_{GLINT}, is strongest during when glint is present and the neural network output, O_S, is positive only when the target is present. For this simulation, a weight of 1 was used for W_{SN}, a weight of 2 was used for W_{GLINT}, and a bias of -1.5 was used for O_S.

4 Simulation

A simulation was performed to evaluate the two-layer neural network against the algorithm based around traditional signal processing. The simulation consisted of injecting 4000 samples of small arms flash signals with white noise, sun glints signals with white noise, and white noise into each algorithm. See Figure 8 for a representative sample of each type of stimulus. The Matlab code used to perform this simulation is captured in the Appendix. This code is based off a larger small arms fire indication technology and architecture analysis and simulation perform by Symeonidis [4].

If an algorithm declared either a sun glint with white noise or a signal that only has white noise, the detection was recorded as a false alarm. Algorithm thresholds and weights were varied to characterize

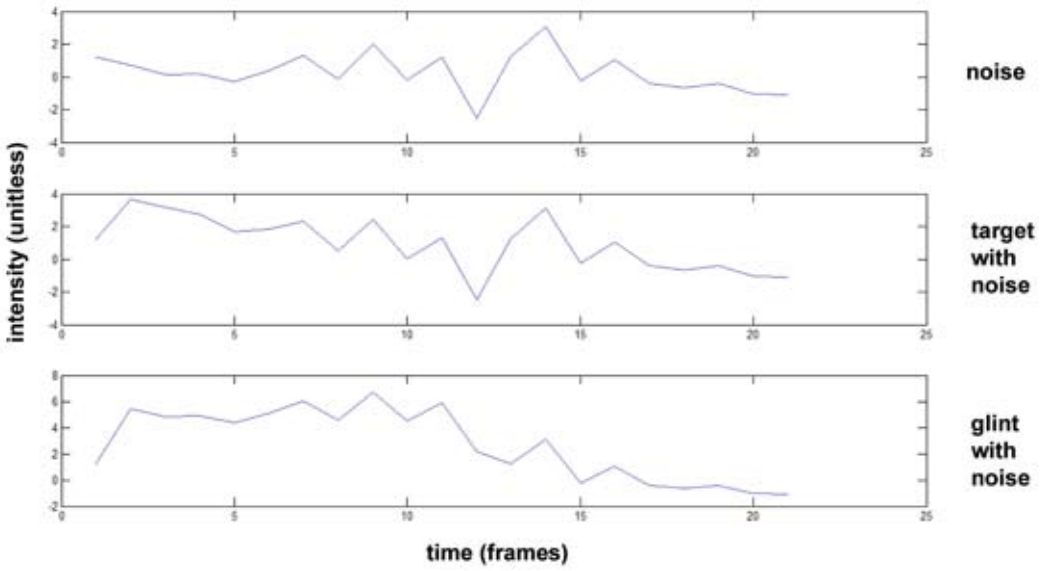

Figure 8: Example Stimuli.

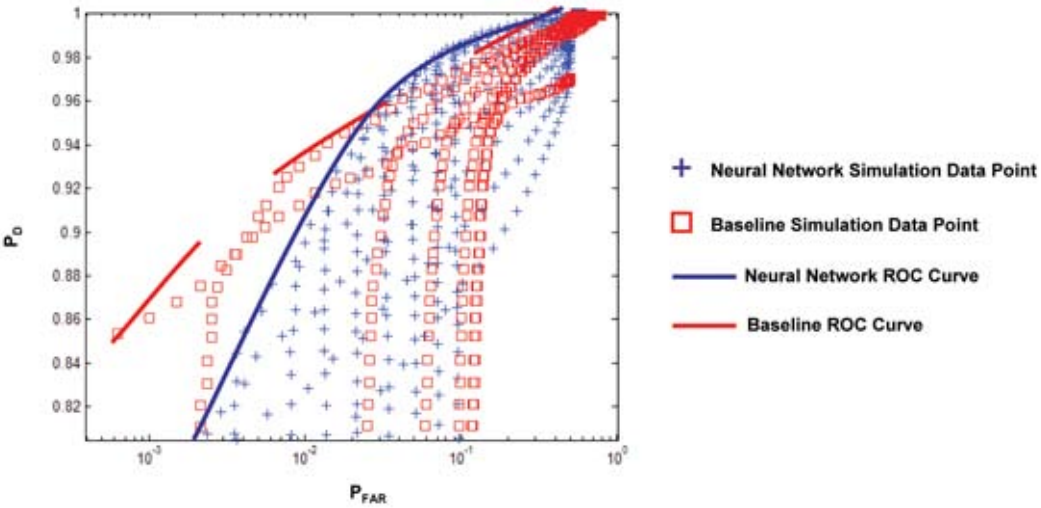

Figure 9: Small arms declaration neural network.

algorithm performance over range, and the results were captured via a Receiver Operating Characteristic (ROC) curve that relates P_D and P_{FAR}. The results of the simulation are captured in Figure 9. The emphasis of this work is on systems with both high PD and low PFAR, and consequentially, this graph focuses on this region of the ROC curve. The significant finding from the simulation is that if high P_D, i.e. greater than ninety-five percent, is a requirement, lower P_{FAR} can be achieved using a two-layer neural network. In areas where P_D is diminished, the traditional signal processing algorithm outperforms the neural network. This suggests that the inclusion of the clutter signal and the existence of only one threshold can improve performance. However, the neural-network does not outperform the baseline filter in all conditions. If the emphasis is primarily on minimizing false alarms and the designer is willing to compromise P_D, the matched filters, based on maximizing signal-to-noise (SNR) and signal-to-clutter (SCR) is the better method.

5 Conclusion

The emphasis of this work was identifying an algorithm capable of achieving high probability of detect

while minimizing false alarms for systems detecting signal in noise and known clutter. These algorithms can potentially improve the performance of law enforcement small arms fire indication systems. The improved neural network performance, over an approach based on traditional processing, was achieved because specific clutter phenomena can be filtered out and a second-layer neuron, which performs a weighted sum, can reduce the number of threshold used to separate signal from noise and clutter from two to one. This is significant since it allow for reliable system operation, i.e. systems with high P_D and low P_{FAR}, i.e. the top-right portion of the ROC curve.

Outside performance, another positive aspect is that the architecture can be easily expanded to detect other temporal events, perform classification/identification, and further reduce P_{FAR} by filtering other temporal clutter sources. If the target and clutter signatures are not known, or vary considerably, the neural network can also be trained using representative data. Another advantage is this neural network can be implemented using only three weighted sum whereas the baseline algorithm a similar number and type of operations and one divide (see Equation 6). Divides can be significant because they can occupy more processing resources/bandwidth and do not exist in some embedded processors. Overall, neural networks can provide advantages over traditional filters designed to optimize SNR and SCR, provided that the requirements is for high P_D and there is information about the clutter environment that can be incorporated into the processing.

Future work can be the implementation of the small arms fire indication neural network, specified in this article, in a real-time law enforcement system. This system can be used to evaluate whether the detection and discrimination neural network can operate with data captured from diverse environments, each containing unique temporal clutter. Once the approach has been proven, an analog implementation of this neural network can be integrated with the processing to develop a low impact, i.e. cost, size, weight, and power, electro-optical small arms fire indication system. The advantage of this neural network is that it can easily be implemented using a small number of common analog circuits and lends itself to processing that can be embedded within a sensing element. This may be the realization of the high-altitude surveillance and potentially hostile local-engagement systems discussed in the introduction section [4].

References

[1] Boyer, E. L., 1990. Scholarship Reconsidered: Priorities of the Professoriate, The Carnegie Foundation for the Advancement of Teaching, Princeton, NJ.

[2] Caulfield, J. et.al.,1006. Performance of the Vectored Infrared Personnel Engagement and Return Fire (VIPER) IRFPA Muzzle Flash Detection System. Proc IRIS Specialty Group in Passive Sensors, 1996.

[3] RAFAEL Small Arms Detection System (Israel), Threat warning systems. http://www.janes.com/articles/Janes-Armour-and-Artillery-Upgrades/RAFAEL-Small-Arms-Detection-System-Israel.html., accessed: June 2009.

[4] Symeonidis, S., 2009. Electro-optical systems and neural-inspired processing: a system architecture and technology analysis with applications to law enforcement small arms fire indication systems. PhD Dissertation, Texas Tech University, Mechanical Engineering, 2009.

[5] Frankel, D., 2001. Assessment of Waco, Texas FLIR Videotape. in Proc SPIE 4370: pp. 286-300.

[6] Scribner, D., et al., 1999. Advanced Focal Planes and Neuromorphic Processing. Meeting of the IRIS (MSS) Specialty Group on Infrared Detectors.

[7] Kramer, J. and G. Indiveri, G., 1998. Neuromorphic Vision Sensors and Preprocessors in System Applications. Advanced Focal Plane Arrays and Electronic Cameras, Bellingham, WA: SPIE Optical Engineering Press.

[8] Callan, C., J. Goodman, J., 2005. Sensors to Support the Soldier. Office of Naval Research, Arlington, VA, Rep. JSR-04-210.

[9] Marchant-Smith, D., Haslem, P. R., and Smith, C. J. M., 1982. Small Arms and Cannons, Oxford: Brassey's Publishers.

[10] Klingenberg, G. and Heimerl, J., 1992. Gun Muzzle Blast and Flash, Reston, VA: American Institute of Astronautics and Aeronautics.

[11] McCluney, W. R., 1994. Introduction to Radiometry and Photometry. Boston: Artech House Publishing.

[12] Grant, B. G. and Hardy, D. T., 2001. Muzzle Flash Issues Related to the Waco FLIR Analysis. Proc SPIE, 4370, pp. 314-324.

[13] Spera, T. J. and Figler, B. D., 1997. Uncooled Infrared Sensors for an Integrated Sniper Location System. Proc SPIE, 2938, pp. 326-339.

[14] Luminous Efficacy. www.wikipedia. com, accessed: June 2009.

[15] Hummingbird. www.wikipedia.com, accessed: June 2009.

[16] Night Vision Thermal Imaging Systems Performance Model: User's Manual & Reference Guide, Fort Belvoir, VA: U.S Army Night Vision and Electronic Sensors Directorate Modeling & Simulation Division, 2001.

[17] Sun Fact and Figures. http:// solarsystem.nasa.gov /planets/profile.cfm? Object=Sun&Display=Facts & System=Metric, accessed: June 2009.

[18] Voskoboinik, A., 2008. Novel Approach for Low-Cost Muzzle Flash Detection System. Infrared Technology and Applications, 6940:N1-N10.

[19] Rob, F., et. al., 1992. A CFAR Adaptive Matched Filter Detector. IEEE Transactions on Aerospace and Electronic Systems, 28(1), pp.208-216.

About the Authors

Simeon Symeonidis is a systems engineer with 13 years of industry experience. He worked on Application Specific Integrated Circuits (ASICs), Field Programmable Gate Arrays (FPGAs), processor modules, GPU-accelerated software, algorithms, image/signal processing, trackers, and EO/IR designs. He has a Bachelor's Degree in Computer Engineering from Florida Atlantic University, a Master's Degree in System Engineering from National Technological University, and a Doctorate Degree in Mechanical Engineering, with a focus on Transdisciplinary Engineering, from Texas Tech University. This paper is based of his Doctorate research, which was developed while working product development at Raytheon. He now works at Trackingpoint, developing the next-generation embedded trackers and improving upon existing image enhancement algorithms.

Dr. Alan Barhorst is Professor of Mechanical Engineering at Texas Tech University and participates in the Transdisciplinary PhD program there. Dr. Barhorst has served internationally as Mechanical Engineering Program Coordinator for Texas A&M University at Qatar (Doha). Dr. Barhorst has had the opportunity to develop an Engineering degree program centered on Mechanical Engineering but incorporating significant liberal arts curricula for a private liberal arts university in Texas that is exploring expansion of its offerings into engineering. Dr. Barhorst's research interest span traditional Mechanical Engineering fields as well as bridging the disciplines in biology, paleontology, nano-science, and medicine. Dr. Barhorst has industrial experience in aerospace and petroleum industries.

Appendix

Presented in this appendix is the Matlab code used to simulate the baseline and neural network detection and discrimination filters. This code correlates to the Equations 3 - 9 presented in the approach section. This curves presented in Figure 4 was used for the flash_temporal_low input and this script was used to generate Figures 5, 7, and 8 and the ROC performance curve in Figure 9.

```
% Generating signals
for i=1:num_sim
  noise_temporal=wgn(1,21,0); % white Gaussian
  noise
  flash_noise=flash_temporal_low+noise_temporal;
  glint_noise=glint_temporal_low+noise_temporal;


% Performing processing for each signal
  for j=1:3
    if (j==1)
      signal=flash_noise;
  elseif (j==2)
    signal=glint_noise;
  else
      signal=noise_temporal;
  end


  % Baseline processing filters
  signal_detect(i,j)=sum(signal.*flash_filter);
  signal_norm=signal./sum(signal(:));
  signal_discrim(i,j)=sum(signal_norm.*flash_filter);


  % Neural inspired filers
  signal_flash(i,j)=sum(signal.*flash_filter);
  signal_glint(i,j)=sum(signal.*glint_filter);
 end
end
  .
  .
  .
  % Generating baseline ROC curve
  i_count=0; j_count=0;
  for i=low_val_i:inc_i:high_val_i
    i_count=i_count+1;
    detect_thes=signal_detect¿i;
    for j=low_val_j:inc_j:high_val_j
      j_count=j_count+1;
      discrim_thre=signal_discrim¿j;
      baseline= detect_thes+ discrim_thre;
      base_thre=baseline¿1.5;
      PD_base(i_count,j_count)=sum(base_thre(:,1))/num_sim;
      PN_base(i_count,j_count)=sum(base_thre(:,2))/num_sim;
```

```
        PC_base(i_count,j_count)=sum(base_thre(:,3))/num_sim;
        PFAR_base(i_count,j_count)=(PN_base(i_count,j_count)+
                PC_base(i_count,j_count))/2;
    end
end
.
.
.
% Generating ANN Receiver Operating Characteristic (ROC) curve
i_count=0; j_count=0;
for i=low_val_i:inc_i:high_val_i
    i_count=i_count+1;
    signal_bias=signal_flash+i;
    for j=low_val_j:inc_j:high_val_j
        j_count=j_count+1;
        signal_ANN=signal_bias-signal_glint*j;
        ANN_thre=signal_ANN¿0;
        PD_ANN(i_count,j_count)=sum(ANN_thre(:,1))/num_sim;
        PN_ANN(i_count,j_count)=sum(ANN_thre(:,2))/num_sim;
        PC_ANN(i_count,j_count)=sum(ANN_thre(:,3))/num_sim;
        PFAR_ANN(i_count,j_count)=(PN_ANN(i_count,j_count)+
        PC_ANN(i_count,j_count))/2;
    end
end
```